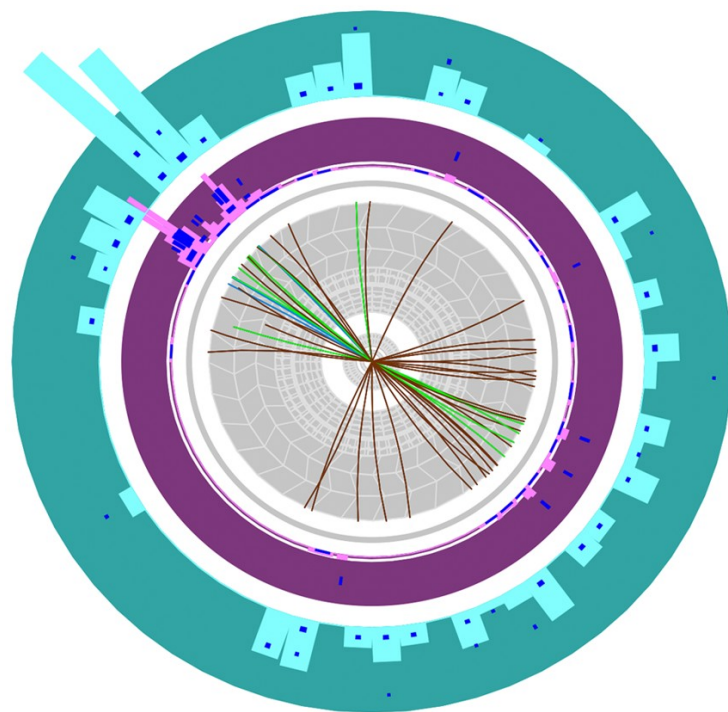


ATLAS results on Heavy Ion Physics



Martin Rybář
for the ATLAS collaboration

*25th Rencontres de Blois:
Particle Physics and Cosmology, May 29, 2013*





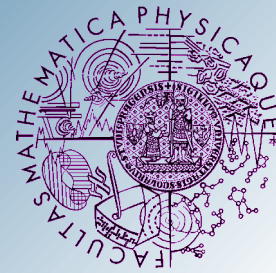
Motivation



- Study of the QCD phase diagram.
- Understanding the bulk properties of the strongly interacting hot medium - Quark-Gluon Plasma (QGP):
 - ◆ Bulk yields
 - ◆ Study of fluctuations
 - ◆ Flow measurement
- How do partons lose energy in QGP?
- ➔ Better understanding of QCD in the limit of high densities and temperatures.
- How does the medium modify the parton showers?
 - ◆ High momentum charged particles yields.
 - ◆ Measurement of jet yields and jet properties.
 - ◆ Electroweak probes and their correlations with jets.



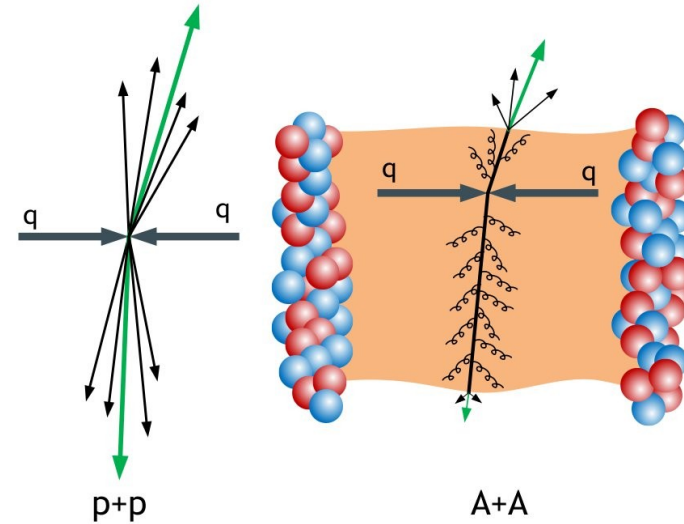
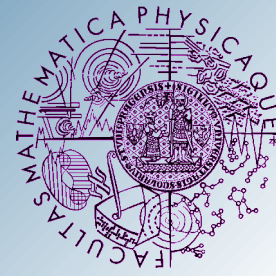
Motivation



- Study of the QCD phase diagram.
 - Understanding the bulk properties of the strongly interacting hot medium - Quark-Gluon Plasma (QGP):
 - ◆ Bulk yields
 - ◆ Study of fluctuations
 - ◆ Flow measurement
- } Yesterday plenary presentation
by Silvia Masciocchi
- How do partons lose energy in QGP?
 - ➔ Better understanding of QCD in the limit of high densities and temperatures.
 - How does the medium modify the parton showers?
 - ◆ High momentum charged particles yields.
 - ◆ Measurement of jet yields and jet properties.
 - ◆ Electroweak probes and their correlations with jets.



Motivation

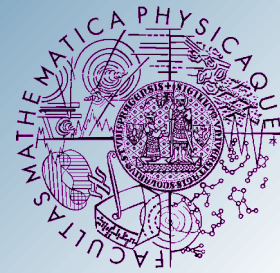


Hard probes:

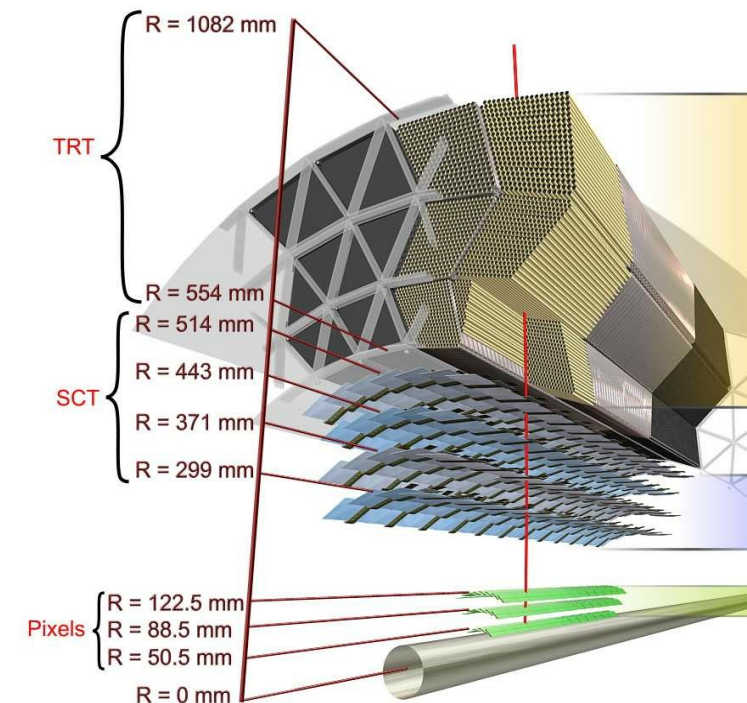
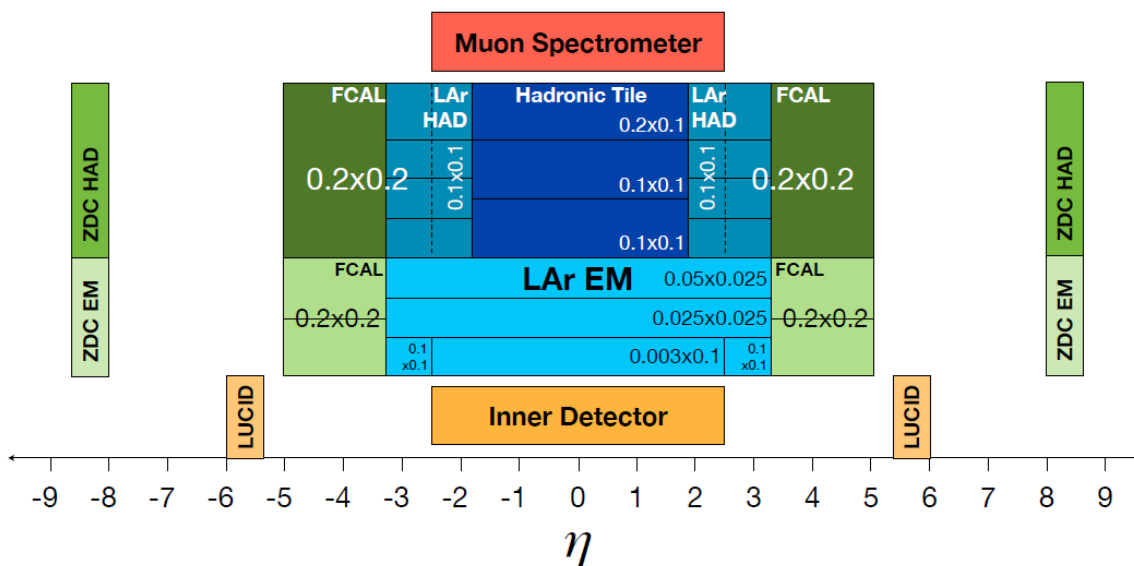
- How do partons lose energy in QGP?
- ➔ Better understanding of QCD in the limit of high densities and temperatures.
- How does the medium modify the parton showers?
 - ◆ High momentum charged particles yields.
 - ◆ Measurement of jet yields and jet properties.
 - ◆ Electroweak probes and their correlations with jets.



The ATLAS Detector

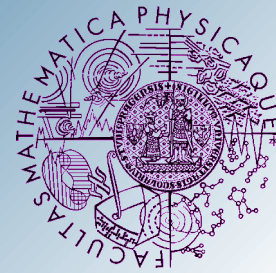


- ATLAS is a general-purpose **p-p** experiment, but it was proven to be well suited also for **heavy ion physics!**
- Large pseudorapidity coverage and full azimuthal acceptance.
- Fine granularity and longitudinal segmentation.
- Precise inner detector in a 2T solenoid field.
- Extensive system of muon chambers placed inside a 1T toroid field.

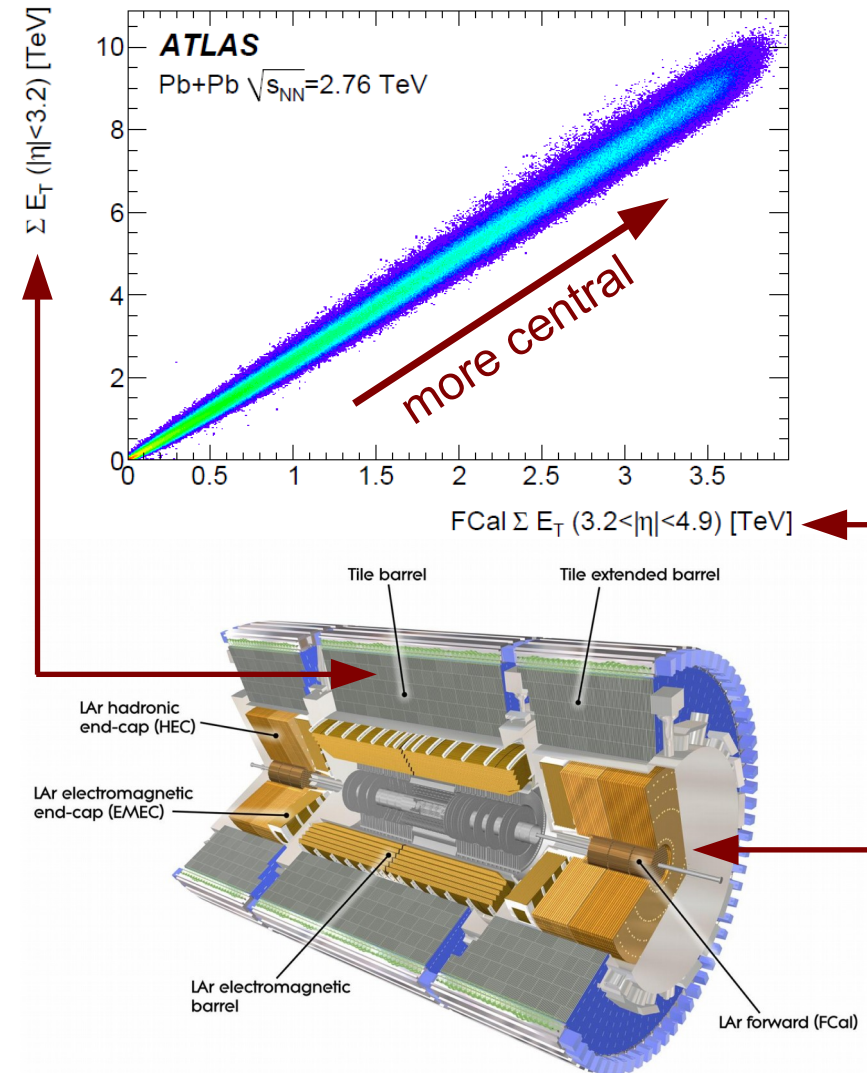
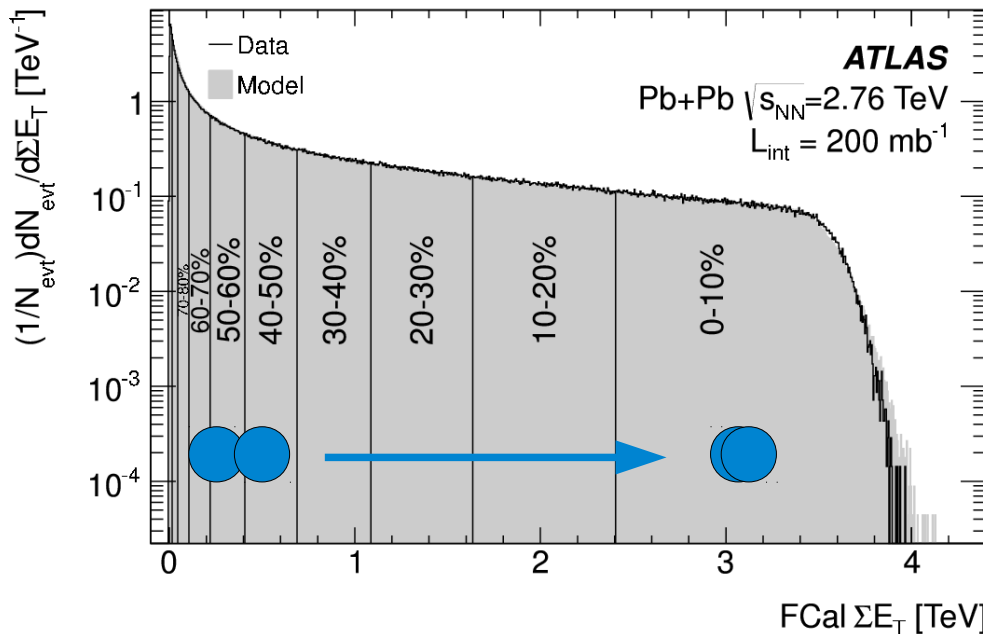




Centrality



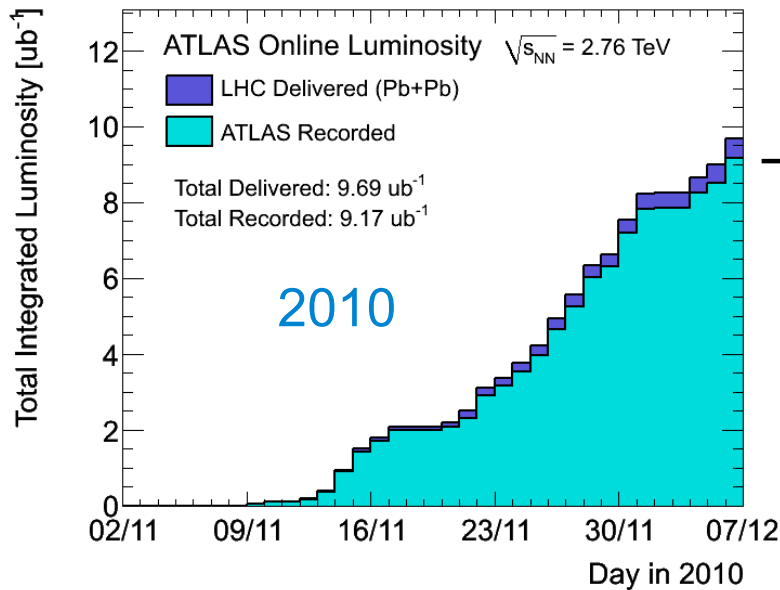
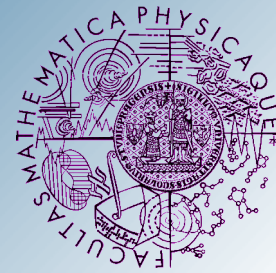
- Characterize centrality by percentile of total cross-section using total E_T .
- Measured in Forward Calorimeter ($3.2 < |\eta| < 4.9$).
- Centrality \rightarrow number of participants N_{part} and binary collisions N_{coll} .



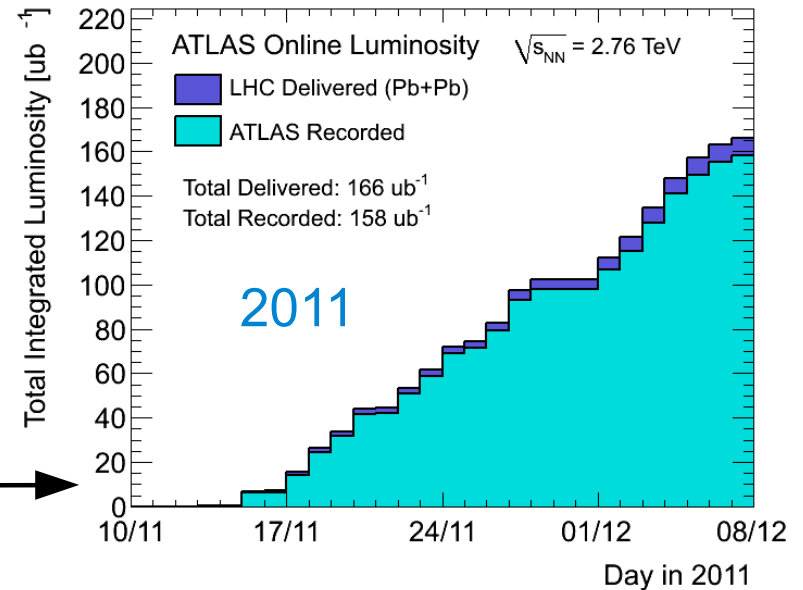
ATLAS calorimeter



Data Sets



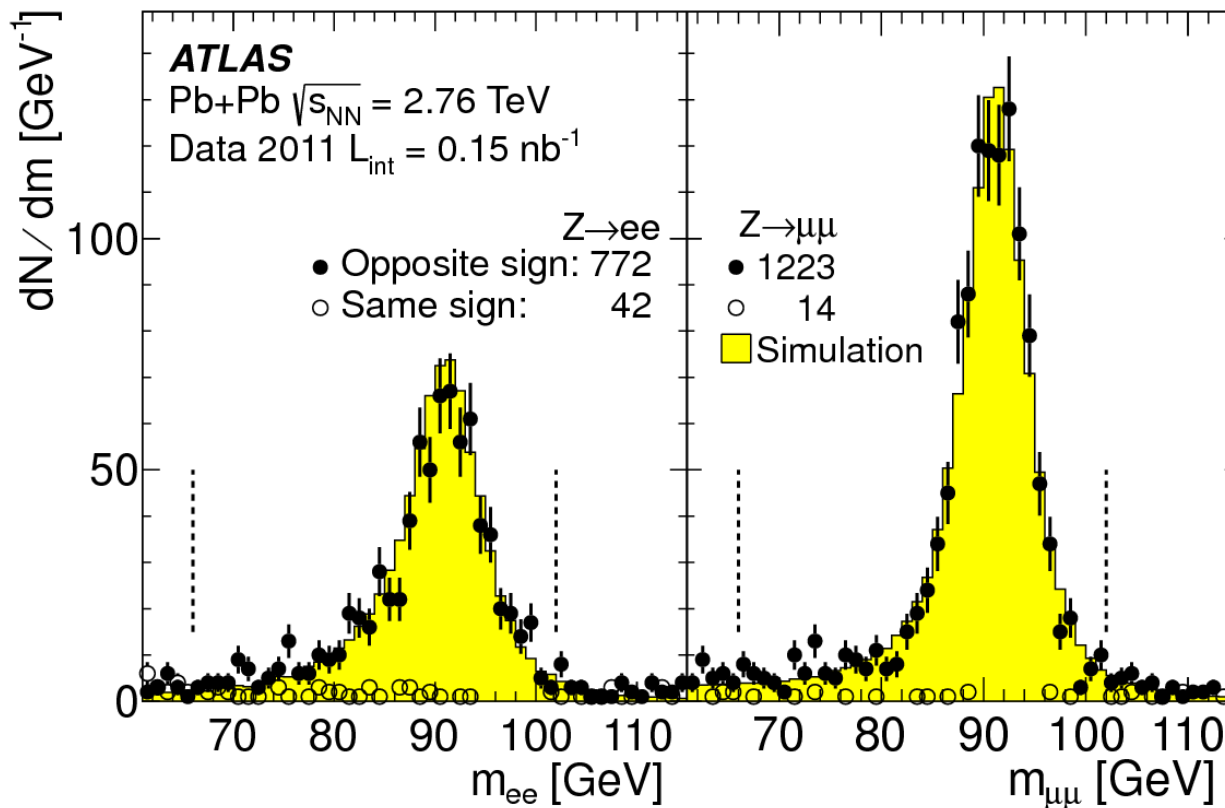
17x more data!



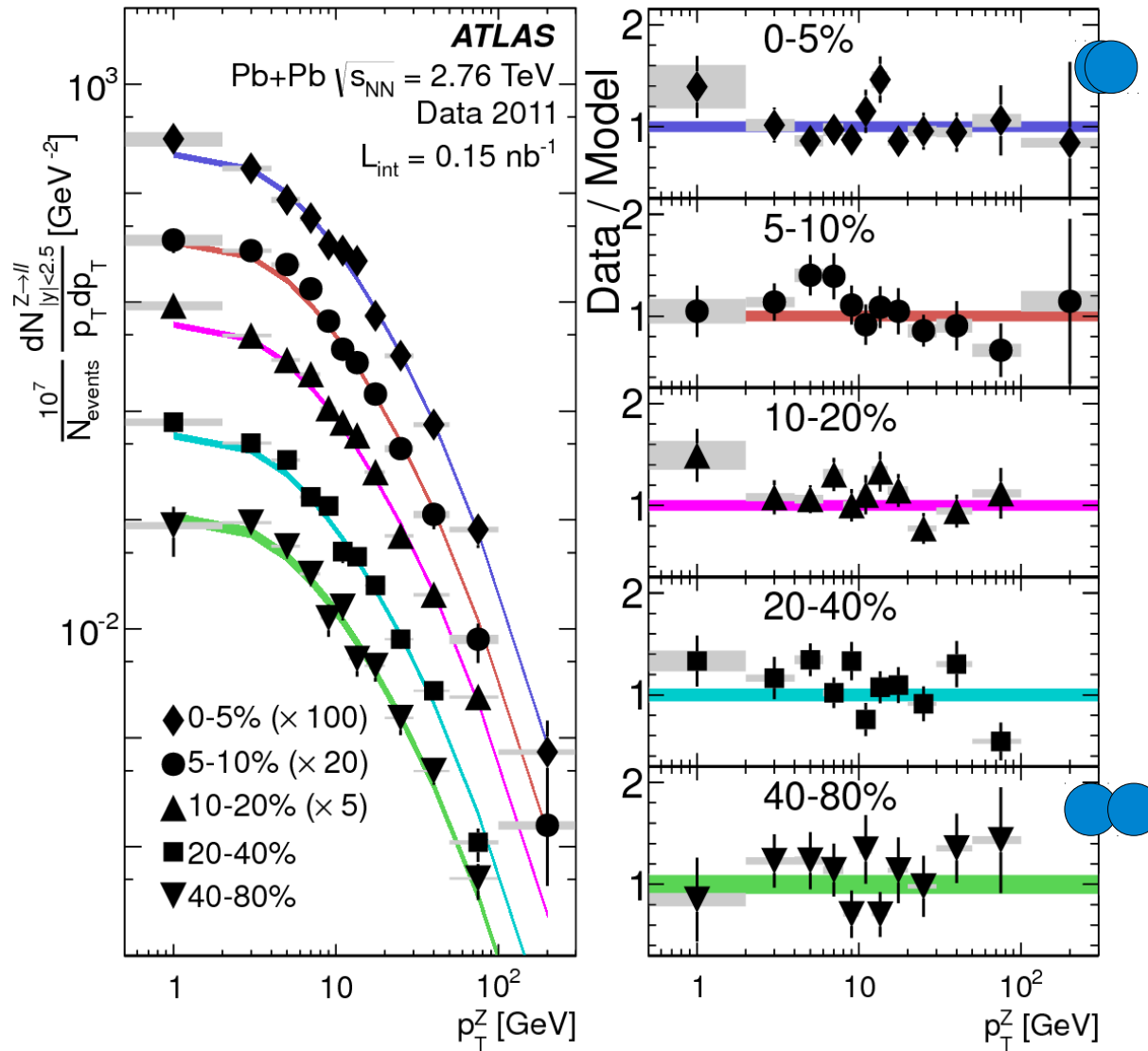
Run:	2010	2011
L_{int}	$8 \mu\text{b}^{-1}$	0.15 nb^{-1}
Triggers	Min Bias	γ , μ , jets, Min Bias, UPC
Nevents	50M	1000M

Electroweak Probes

- Z, W^\pm and photon do not interact strongly with medium.
- ➔ They should obey scaling with number of binary collisions N_{coll} .
- ➔ Their production rate is a standard candle for other processes.
- Test of nuclear PDFs.

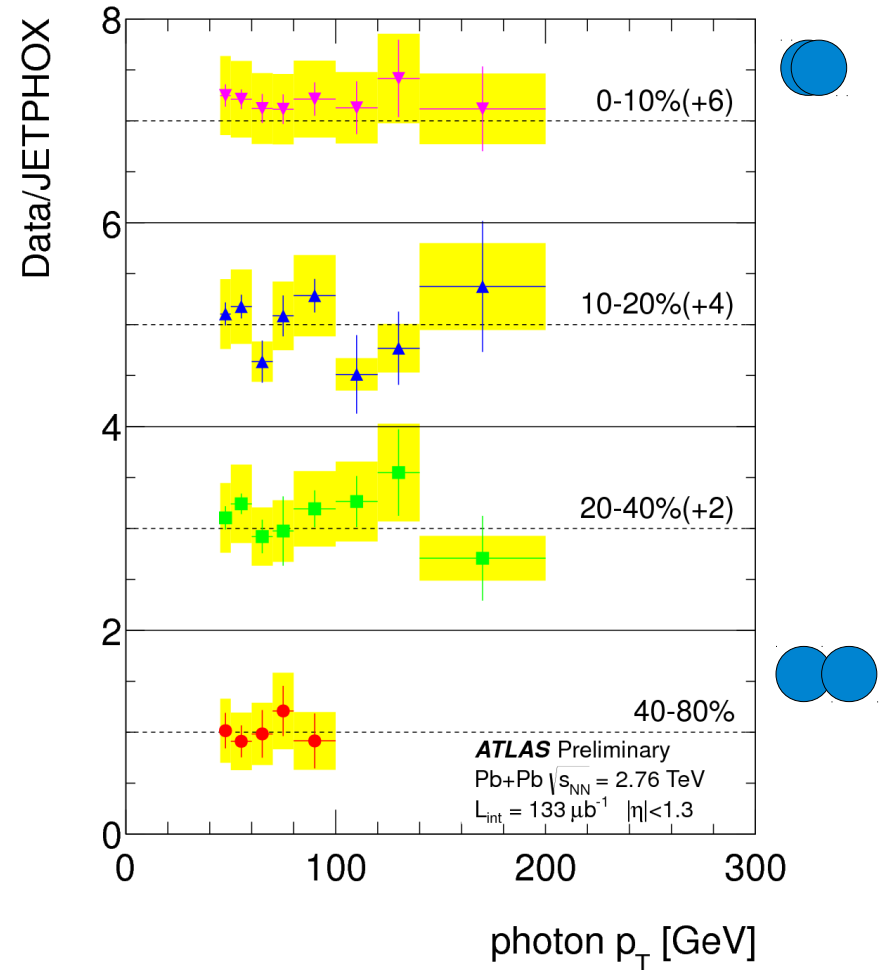
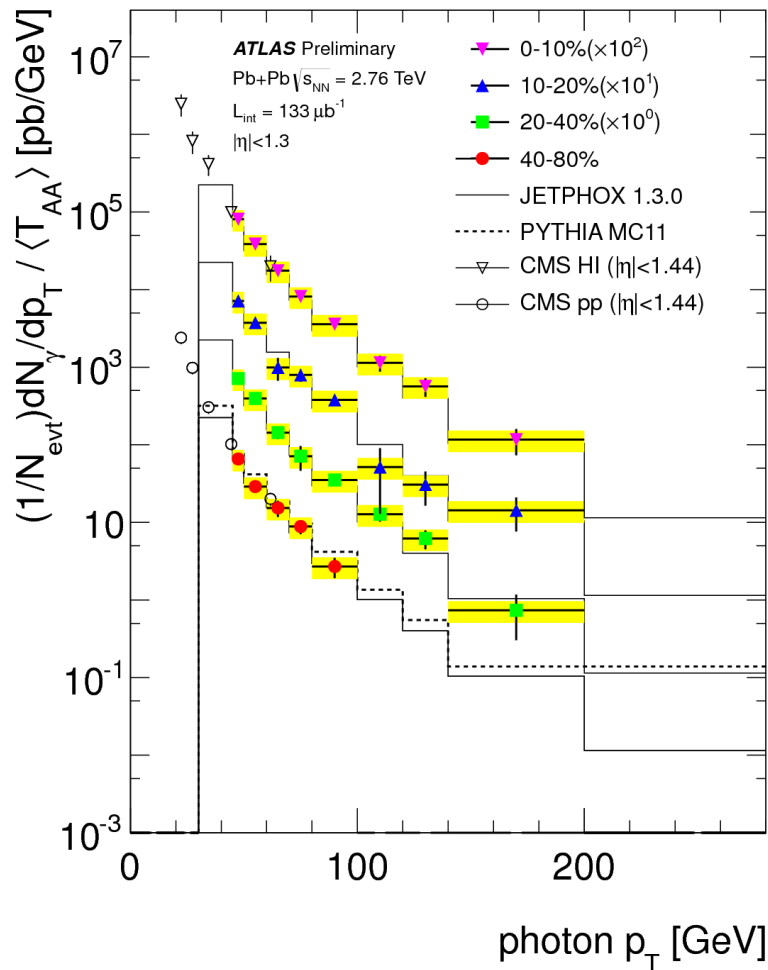


Z Boson Production



- Corrected for efficiency of the reconstruction
- Compared to the PYTHIA with NNLO cross-section simulation scaled by T_{aa}
- ➔ Yields consistent with N_{coll} scaling

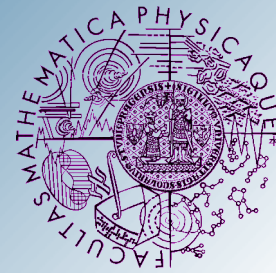
Prompt Photon Production



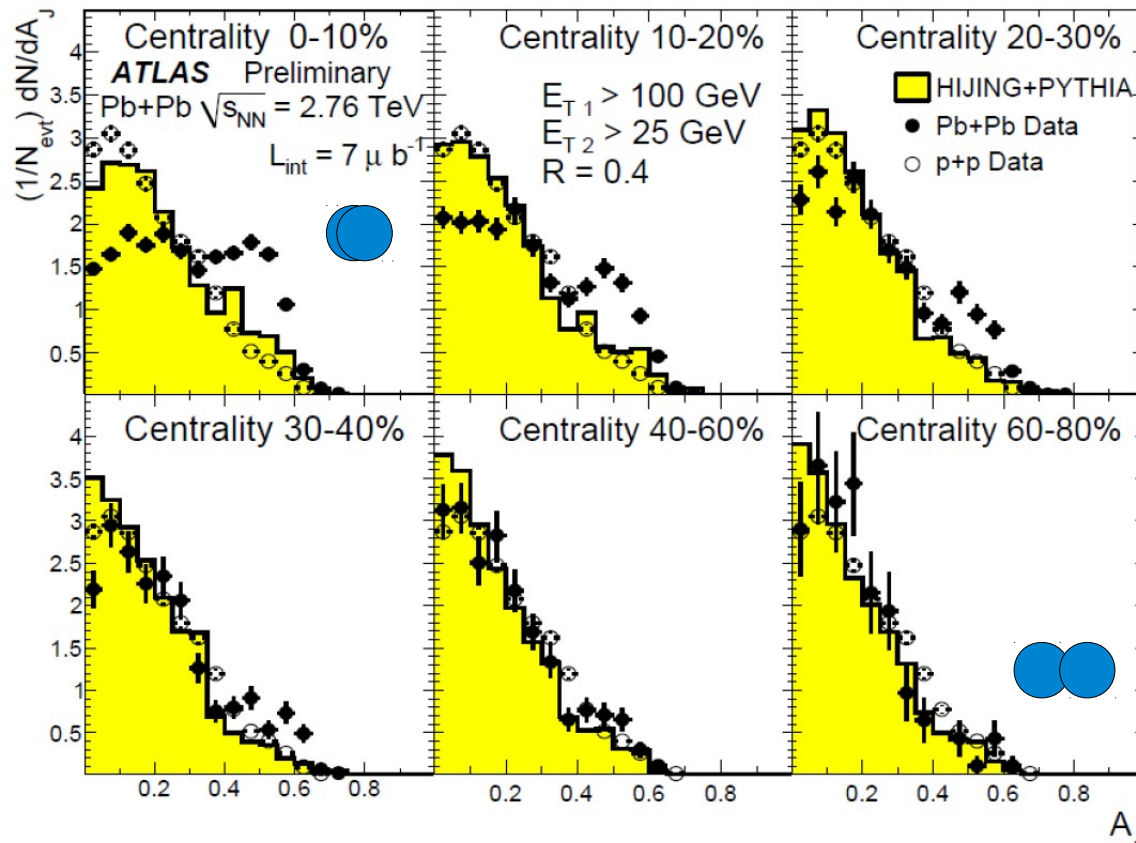
- Photons are UE subtracted.
- Compared to the JETPHOX simulation scaled by T_{aa} .
- Yields consistent with N_{coll} scaling.



Di-jet Analysis



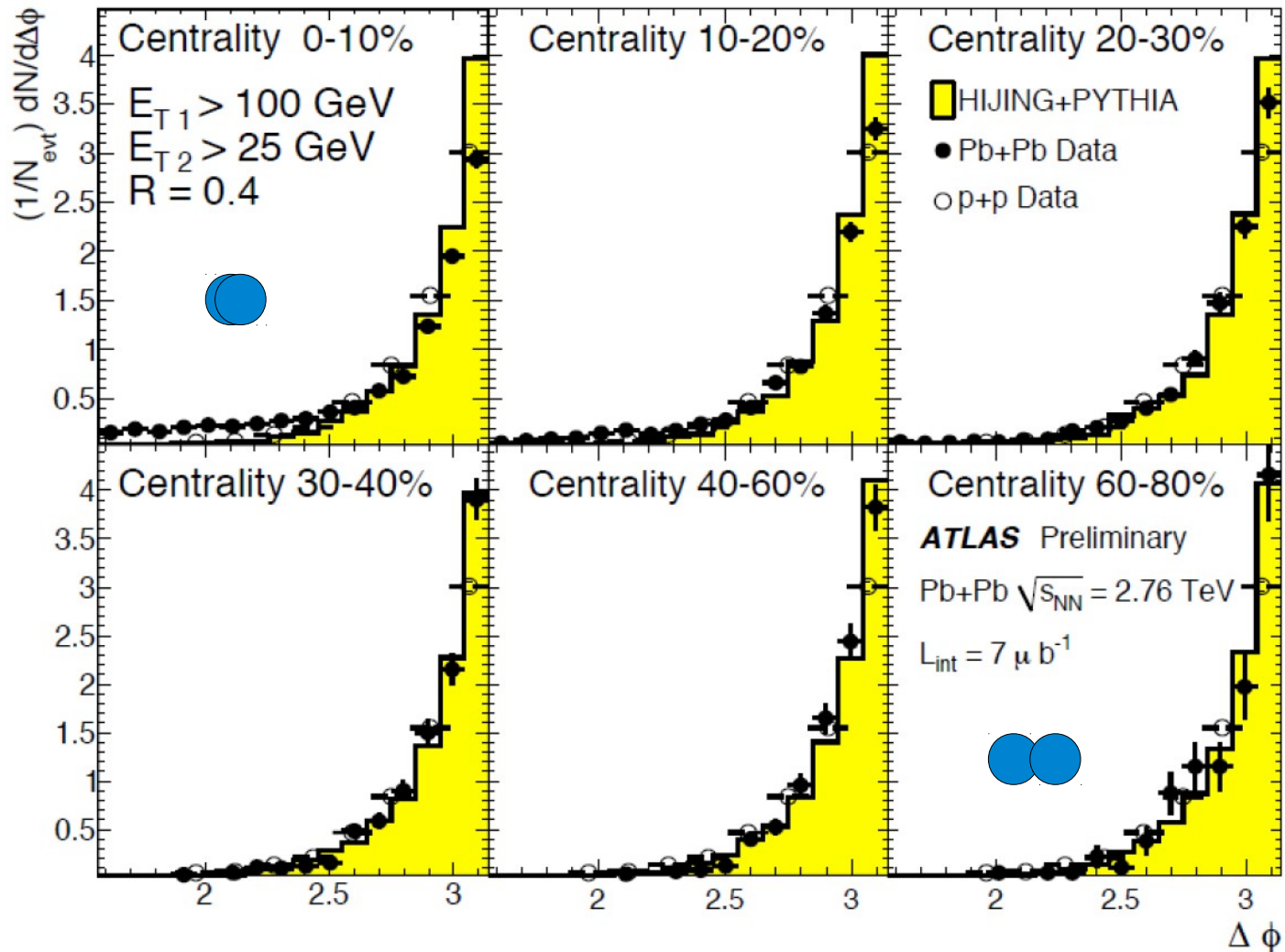
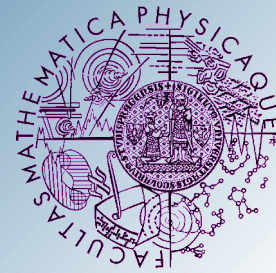
- Dijet imbalance quantified by **asymmetry** variable:
$$A_J \equiv \frac{E_{T1} - E_{T2}}{E_{T1} + E_{T2}}$$
- Leading jet: $E_{T1} > 100$ GeV, $|\eta| < 2.8$.
- Sub-leading jet: highest E_T jet in opposite hemisphere: $\Delta\phi_{12} > \pi/2$, $E_{T2} > 25$ GeV, $|\eta| < 2.8$



Increasing asymmetry with increasing centrality.

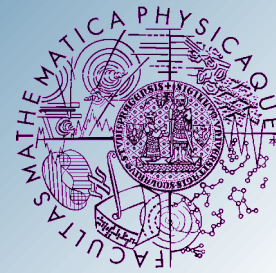


Di-jet Analysis: $d\phi$ Distribution



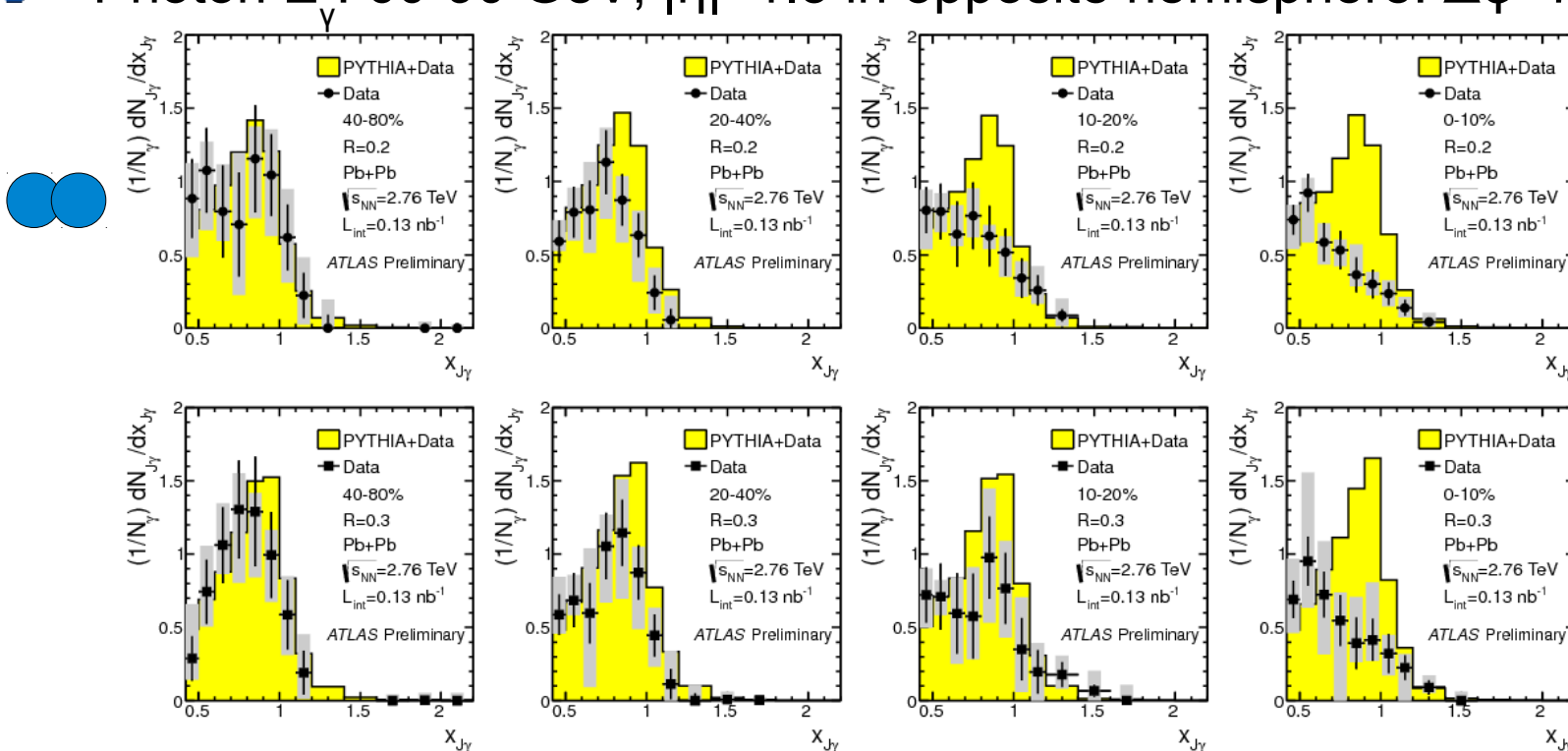


Photon-jet Correlations



- Energy of a parton is calibrated by the energy of photon.
- Large cross-section, purity 75-85%
- Jet: $p_T > 25$ GeV, $|\eta| < 2.1$.
- Photon E_γ : 60-90 GeV, $|\eta| < 1.3$ in opposite hemisphere: $\Delta\phi > 7\pi/8$

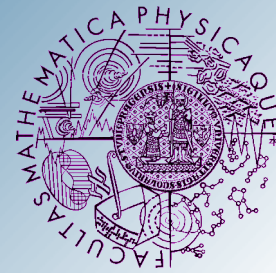
$$X_{J\gamma} \equiv \frac{p_T^{jet}}{p_T^\gamma}$$



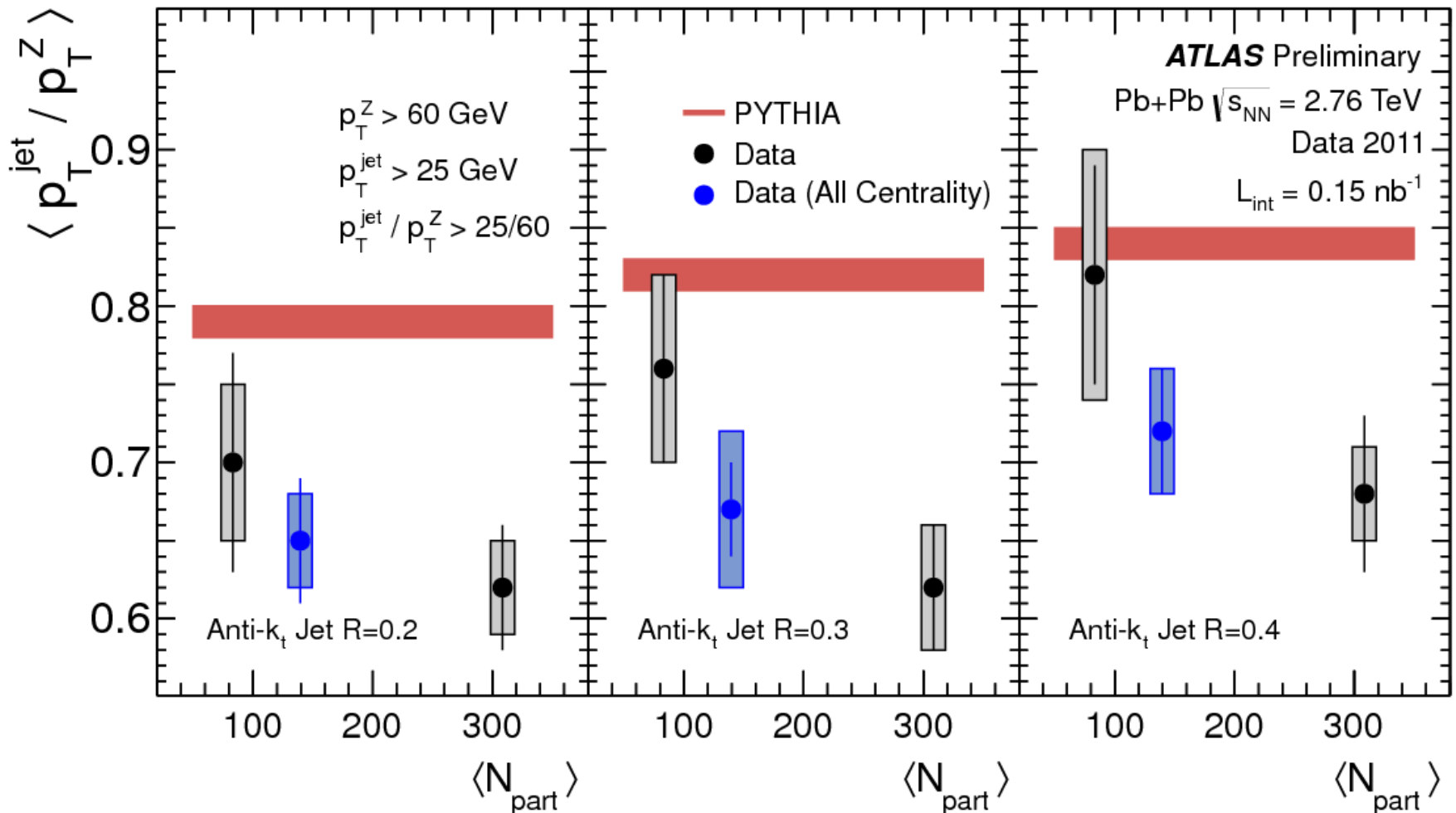
- Good agreement with PYTHIA in peripheral collisions.
- Shift towards smaller $x_{J\gamma}$ and reduction of the integral in central collisions.



Z-jet Correlations



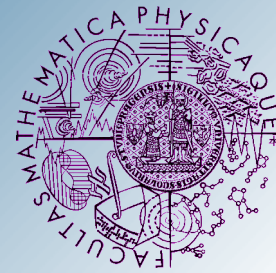
- $Z \rightarrow e^+e^-, \mu^+\mu^-$: $p_T^Z > 60$ GeV in opposite hemisphere: $\Delta\phi > \pi/2$



- Similar observation as in photon-jet correlation but with limited statistic.



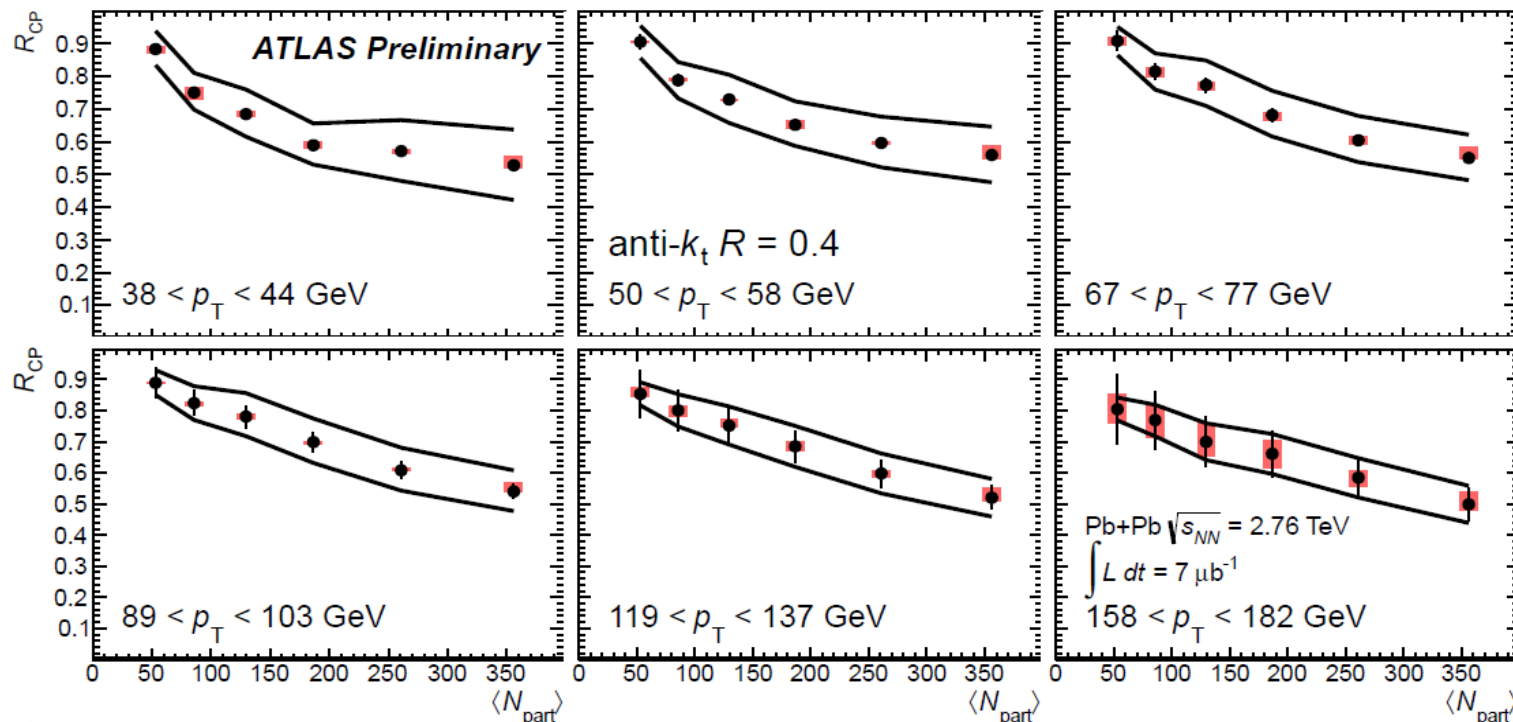
Physics of Jet Quenching



- Measurement of inclusive jet production is another way to study QGP.
- The jet suppression is quantified by central to peripheral ratio:

$$R_{CP} = \frac{1/N_{coll}^{cent} \frac{1}{N_{evnt}^{cent}} dN/dE_T}{1/N_{coll}^{periph} \frac{1}{N_{evnt}^{periph}} dN/dE_T}$$

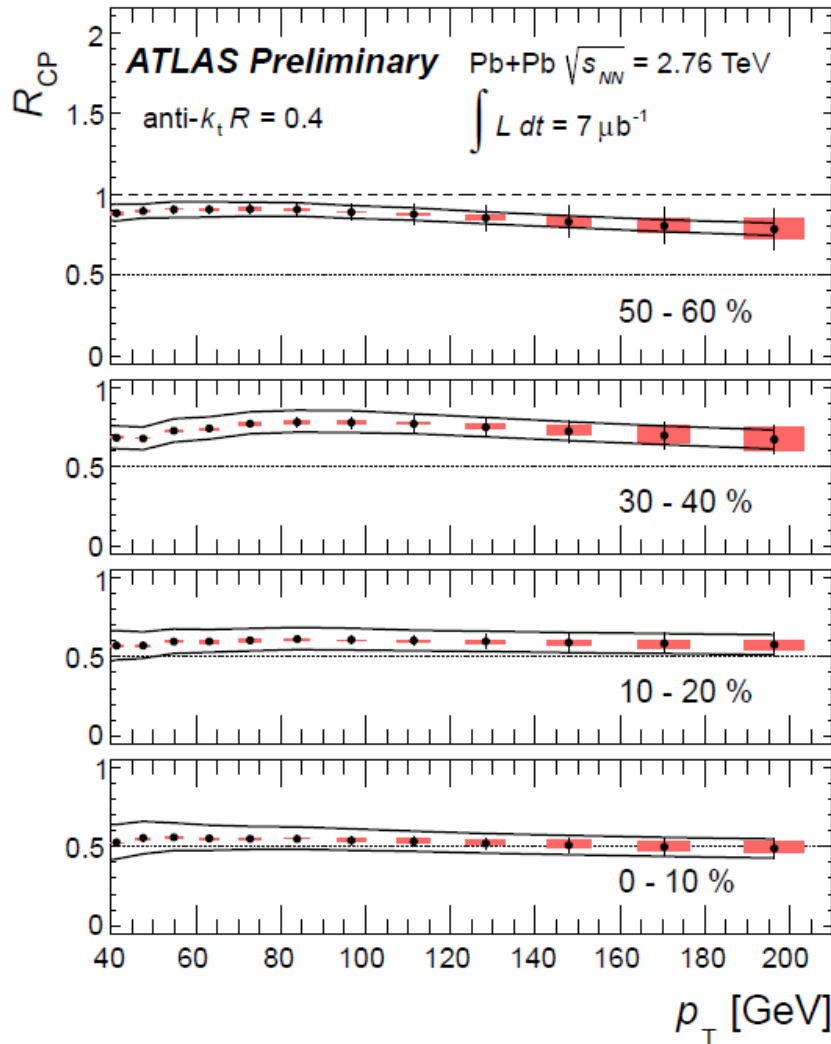
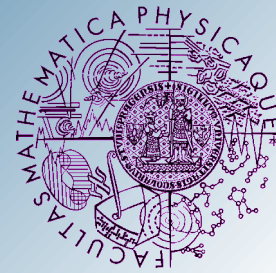
- Some predictions of radiative energy loss suggest that energy can be recovered by expanding the jet cone.



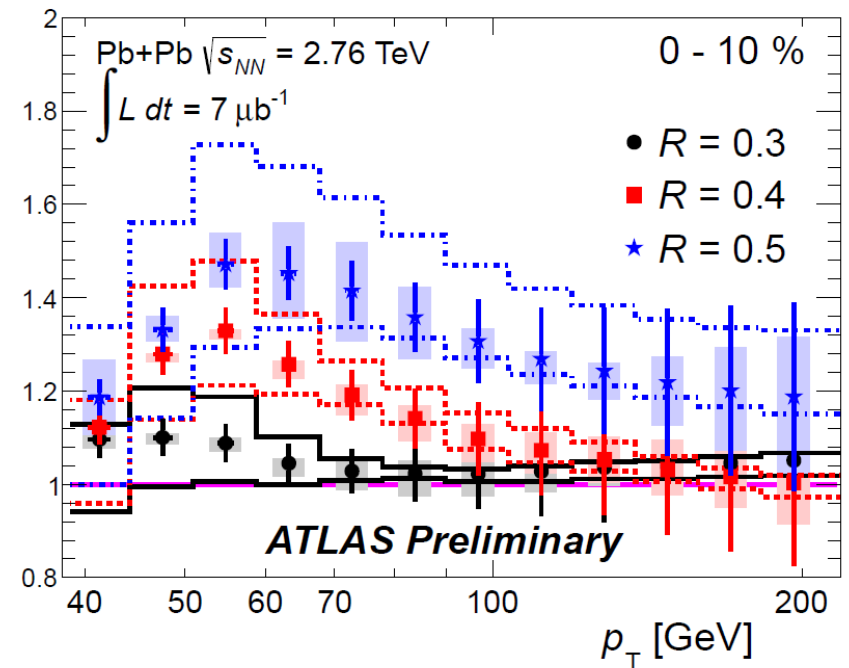
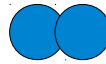
- ➔ Factor of 2 suppression in central with respect to peripheral collisions.
- ➔ The increase is linear for high p_T , quick turns on at low p_T .



Jet R_{CP} as a Function of Jet Radius and Jet p_T



$R_{CP}^R / R_{CP}^{0.2}$

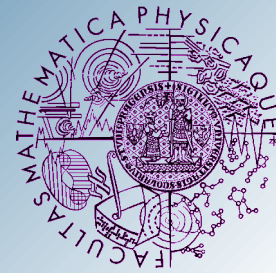


➔ The jet suppression factor shows small variation with the jet p_T .

➔ Less suppression for jets with larger R .

➔ The dependence is more pronounced at lower p_T .

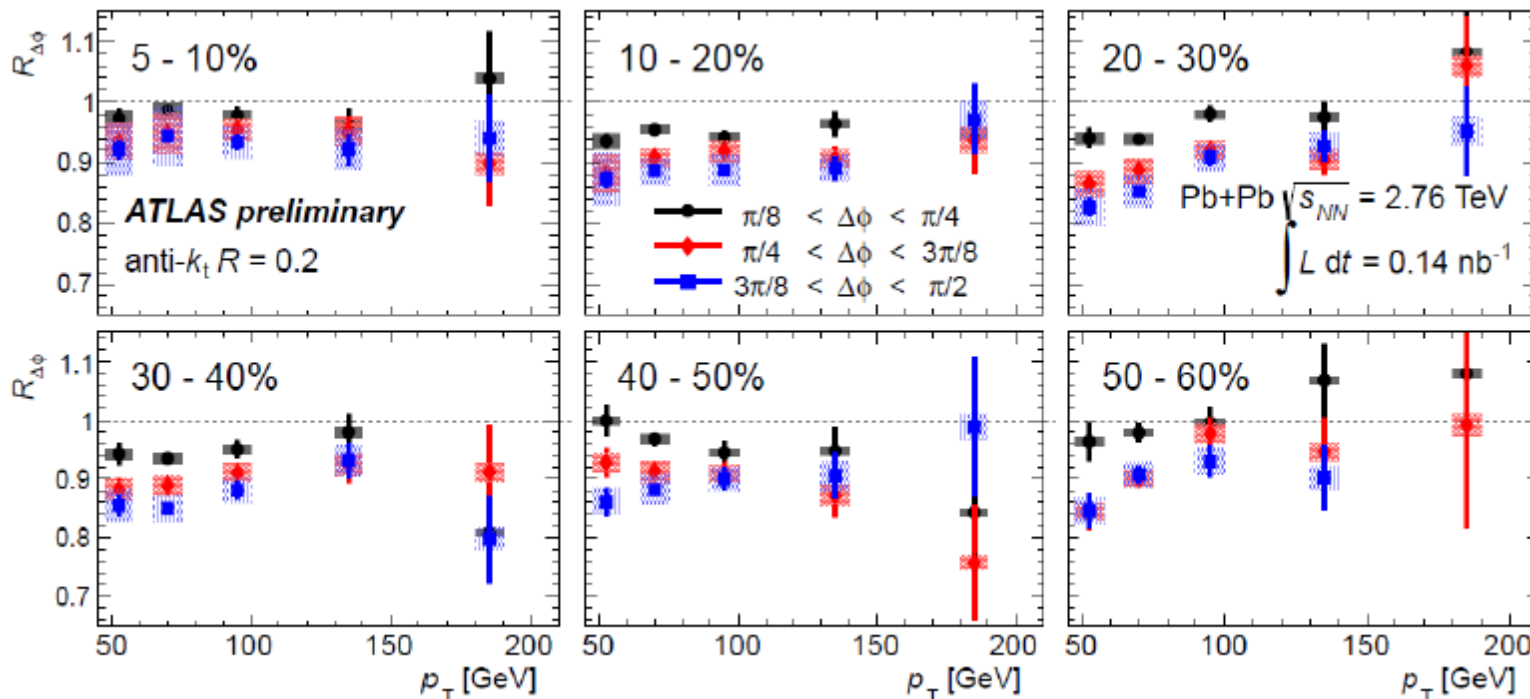
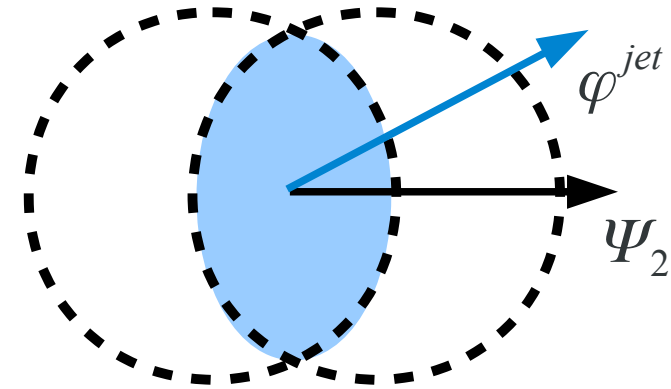
➔ Qualitatively consistent with theoretical calculations.



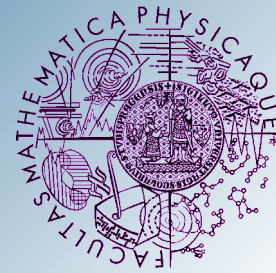
Azimuthal dependence of jet yields

- Path length dependence of jet suppression
- Ratios of yields in different slices of

$$\Delta\varphi = \varphi^{jet} - \Psi_2 \quad \text{with respect to } \Delta\varphi = 0 - \pi/8$$



➡ ~15% reduction in plane yields with respect to out of plane yields.



Jet Structure

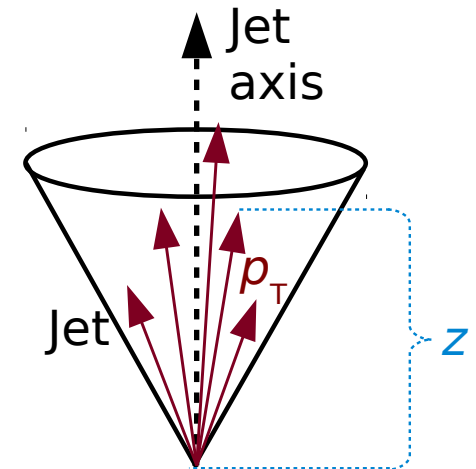
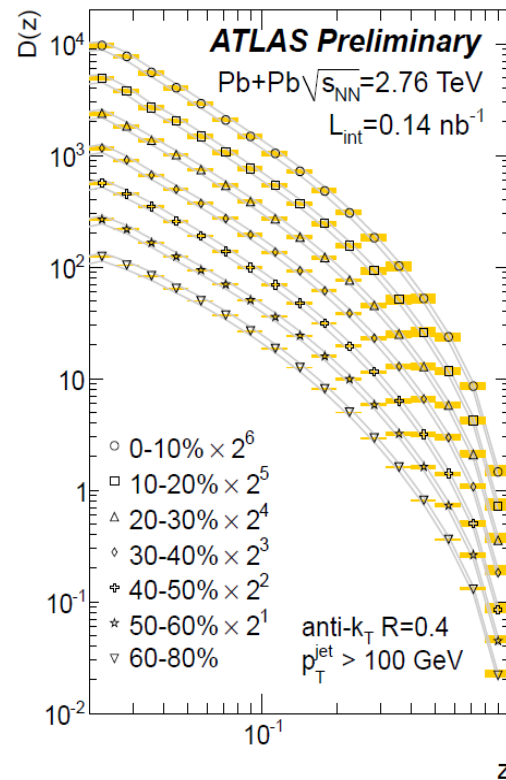
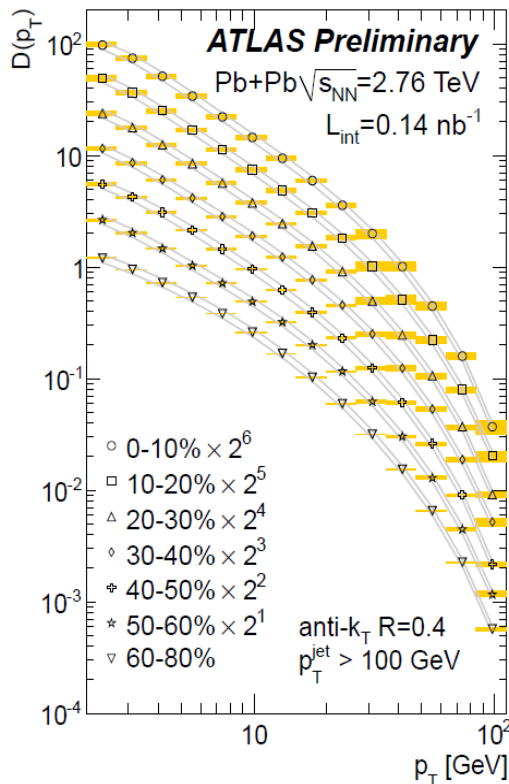
- We measured two sets of fragmentation distributions describing the jet structure:

$$D(p_T) \equiv \frac{1}{N_{\text{jet}}} \frac{1}{\varepsilon} \frac{\Delta N_{\text{ch}}(p_T)}{\Delta p_T} \quad D(z) \equiv \frac{1}{N_{\text{jet}}} \frac{1}{\varepsilon} \frac{\Delta N_{\text{ch}}(z)}{\Delta z}$$

$$z = p_T^{\text{ch}} / p_T^{\text{jet}} \cos \Delta R$$

Spectra of charged particles in jets

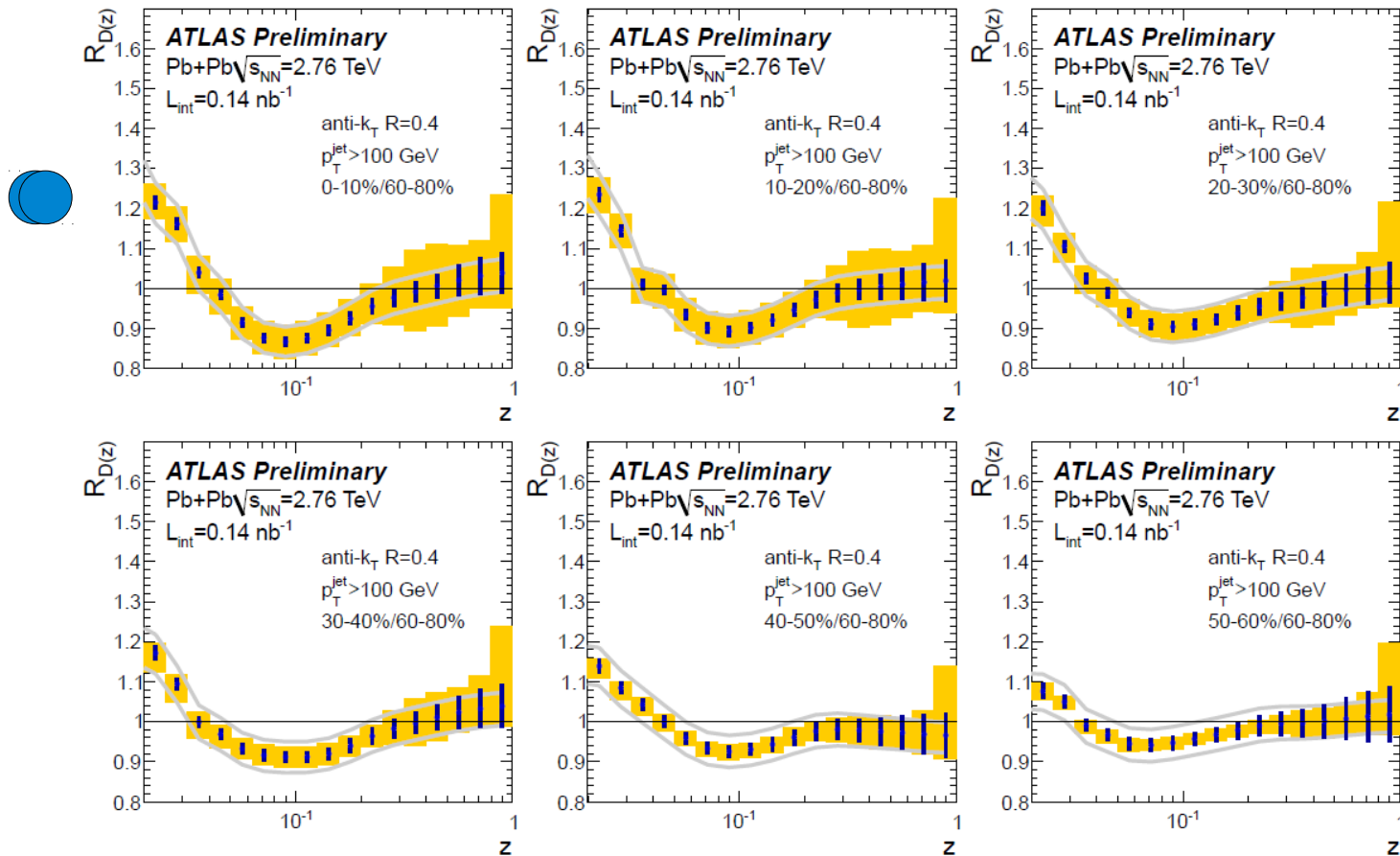
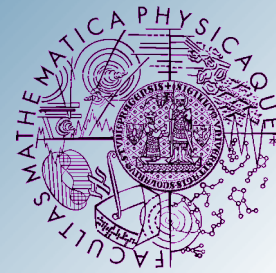
Fragmentation function



- $D(z)$ and $D(p_T)$ distributions have similar shape in all centrality bin.
- ➔ ratios are needed to study centrality dependence.



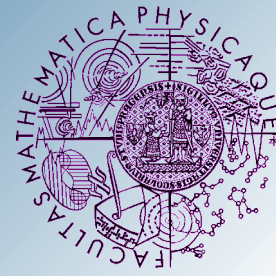
D(z) centrality dependence



- ➔ ~15% suppression at intermediate z (~ 0.1) and 25% enhancement at very low z (~ 0.02).
- ➔ No strong modification at large z (\leftrightarrow leading parton) in central collisions with respect to peripheral ones.



Conclusions



Electroweak probes:

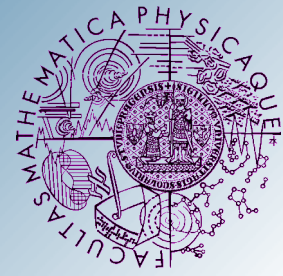
- Z and γ production consistent with N_{coll} scaling

Jets:

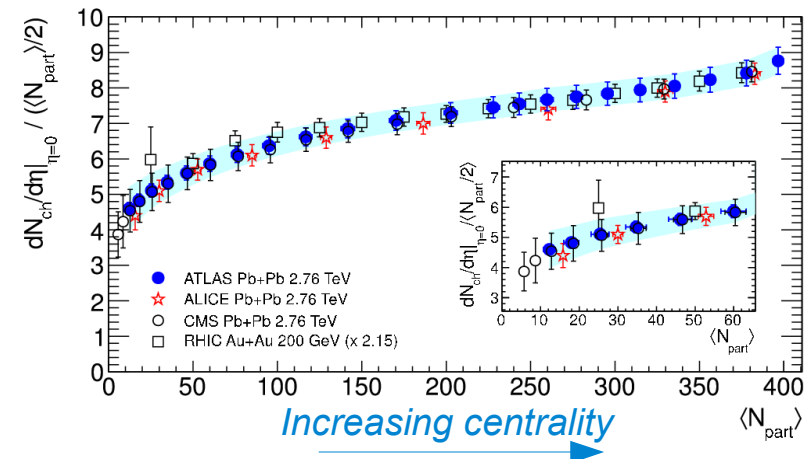
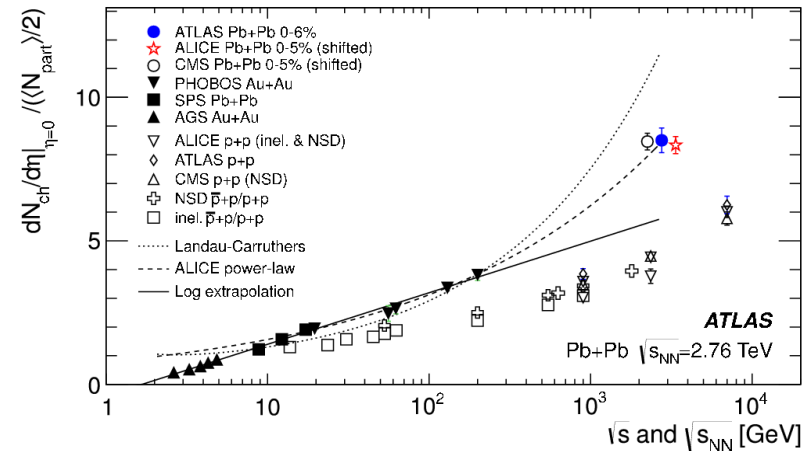
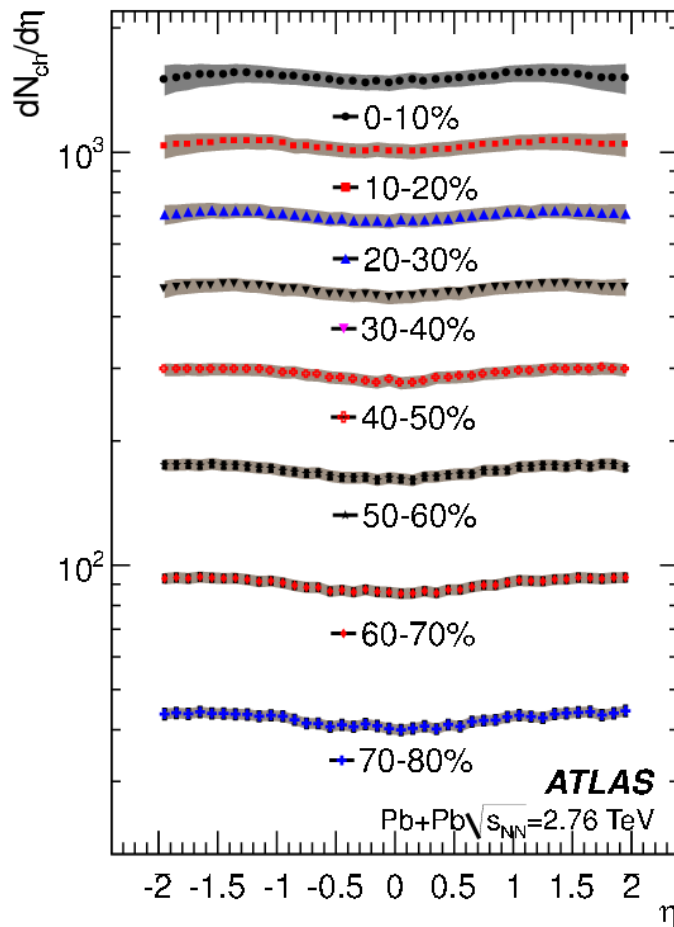
- Energy imbalance in the di-jet, Z-jet and γ -jet system is strongly increasing with increasing centrality.
- Suppression by a factor of 2 is observed in jet yield in central with respect to peripheral collisions.
- The dependence of the jet suppression is very weak on jet p_{T} and jet size except for low p_{T} region.
- Study of jet internal structure shows increasing size of modifications of fragmentation functions with increasing centrality.
- Azimuthal dependence of jet yields exhibits a clear path length dependence.
- Heavy quarks exhibits similar suppression as jets.
- Similar level of suppression observed also in high p_{T} spectra of charged particles.



Backup



Charged Particles Multiplicity

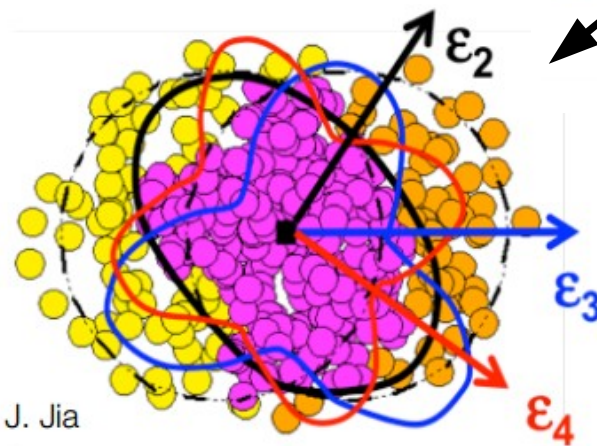
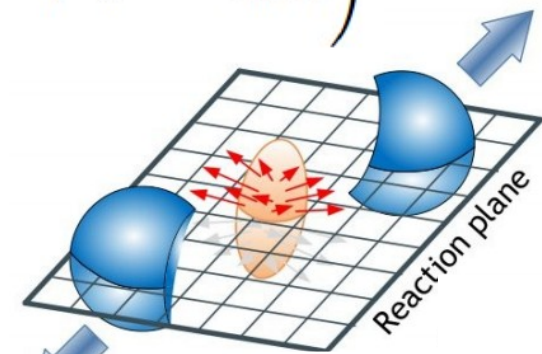


- Yield per participant pair increases by factor of two relative to RHIC with similar centrality dependence.
- Flat in pseudorapidity within $|\eta| < 2$, similarly to p+p.
- Similar centrality dependence as at RHIC → robust scaling feature in HI.

Flow Measurement

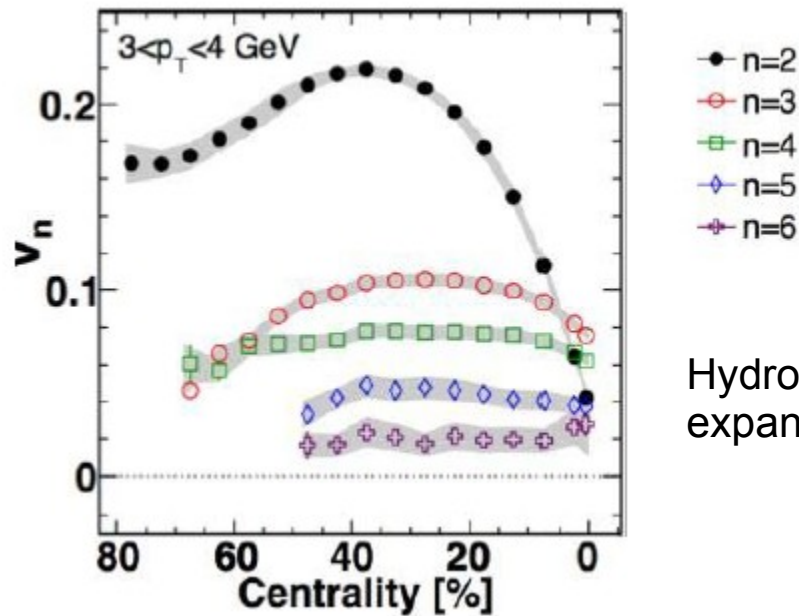
- ➔ Understanding the geometry and bulk properties of the medium.
 - Flow ↔ Particle emission asymmetry due to spatial deformations in the initial overlap region.
 - Studied via Fourier decomposition:

$$E \frac{d^3 N}{dp^3} = \frac{1}{p_T} \frac{d^3 N}{d\phi dp_T dy} = \frac{1}{2\pi p_T} \frac{E}{p} \frac{d^2 N}{dp_T d\eta} \left(1 + 2 \sum_{n=1}^{\infty} v_n \cos [n(\phi - \Phi_{RP})] \right)$$
 - RHIC: mainly measurement of the second and third Fourier coefficient.
 - With the higher multiplicities and larger acceptance ATLAS study higher order components of the flow.

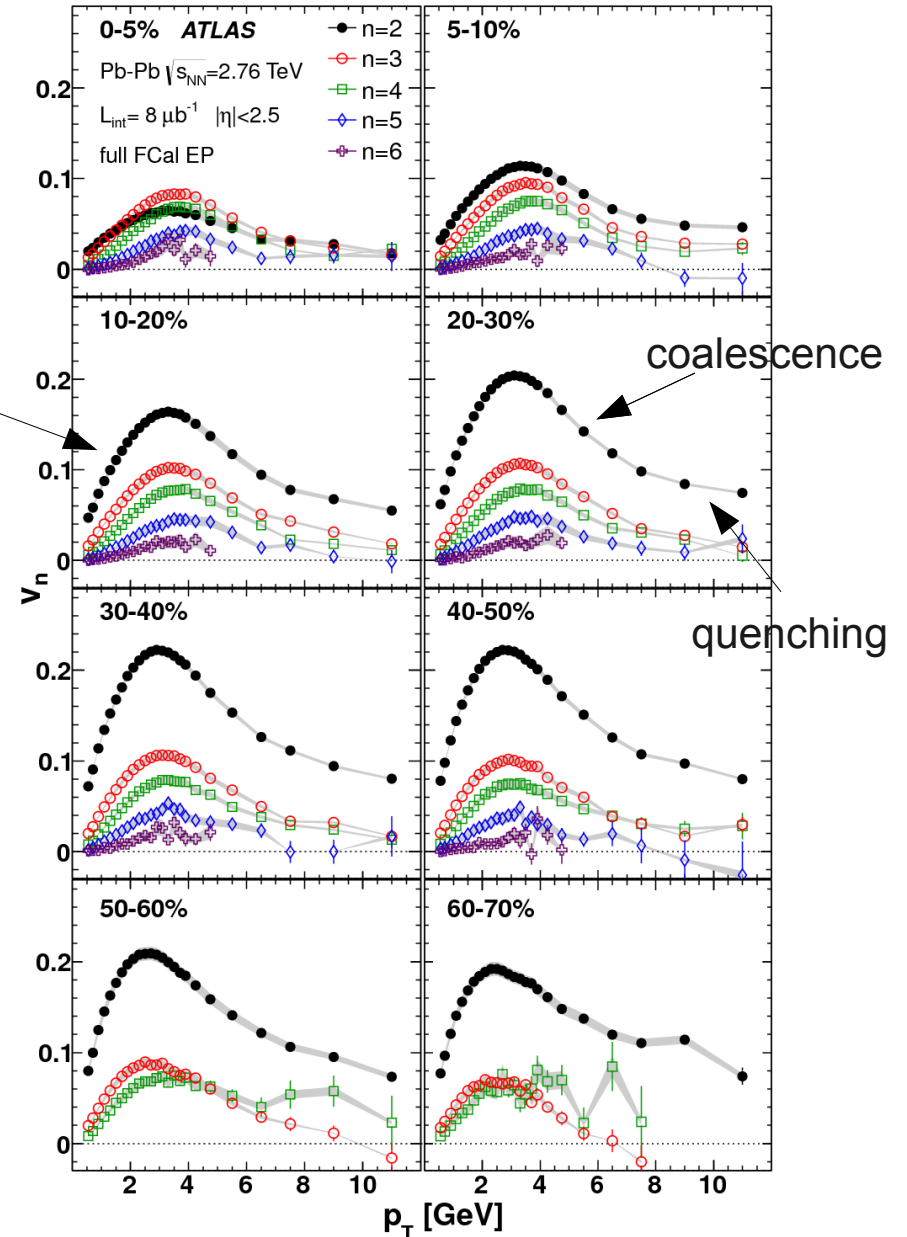


Fluctuations in initial state.

Flow measurement

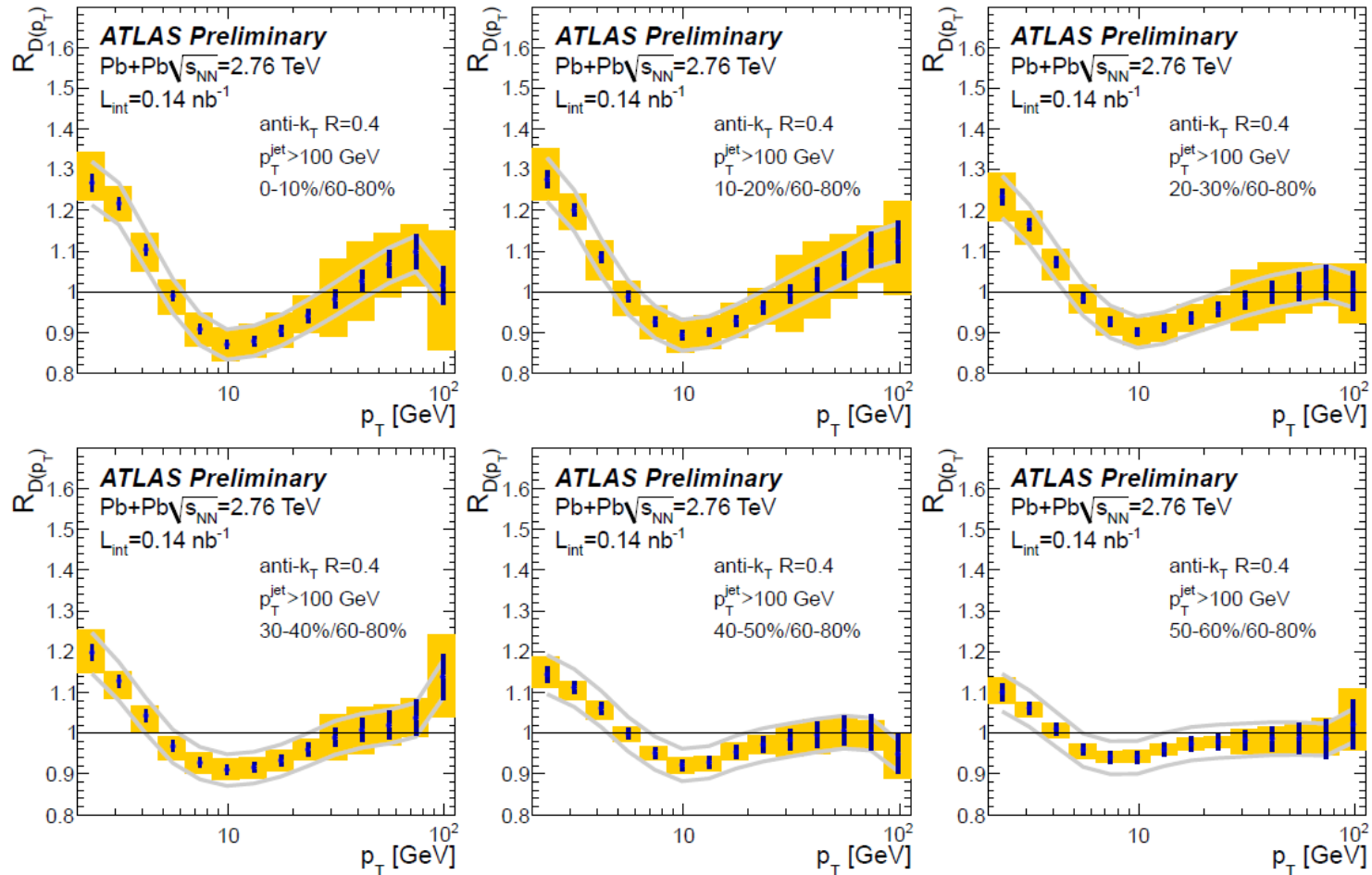
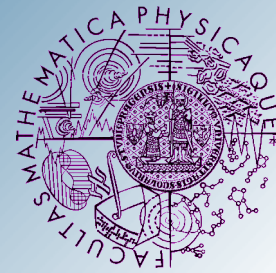


- Similar p_T dependence for v_3 - v_6 .
- Weak centrality dependence observed for v_3 - v_6 .
- For the 5% most central events $v_3 > v_6$.
- No significant η dependence.
- Higher harmonics result from fluctuations of interaction area.





$D(p_T)$ centrality dependence



Shaded bands:
uncorrelated or
partially
correlated
systematic errors

Solid lines:
100% correlated
systematic errors

➡ Similar behaviour as for $D(z)$ distribution.



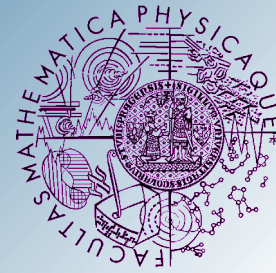
ATLAS Detector Status



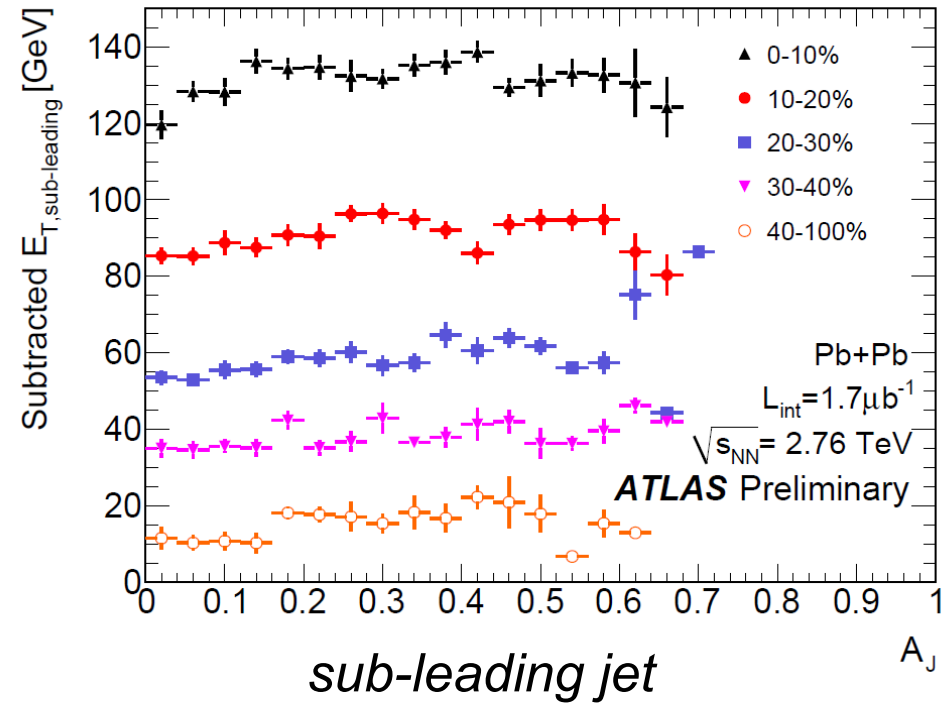
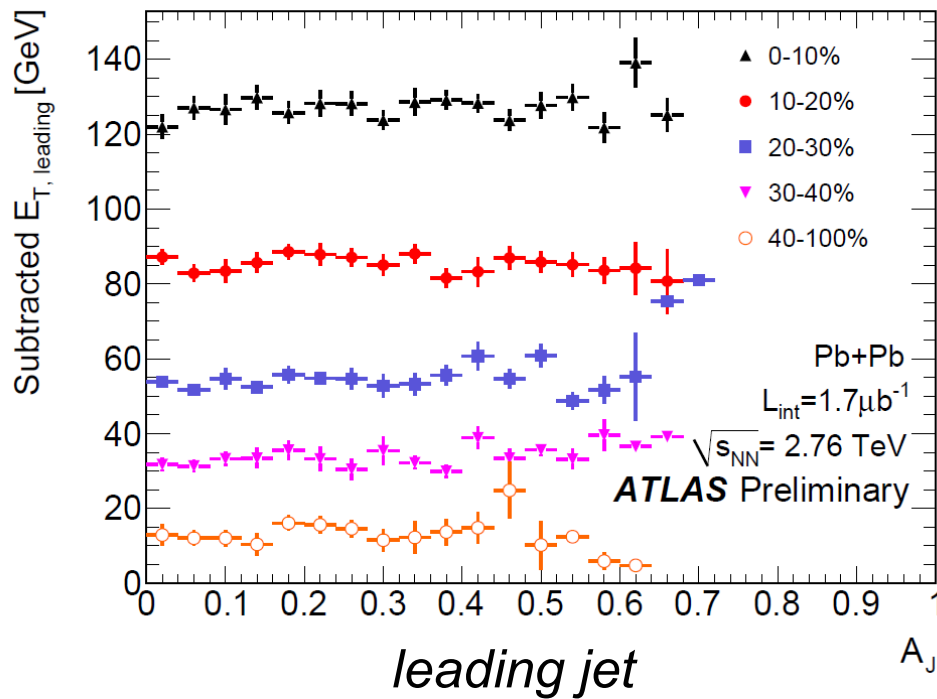
Subdetector	Number of Channels	Approximate Operational Fraction
Pixels	80 M	95.9%
SCT Silicon Strips	6.3 M	99.3%
TRT Transition Radiation Tracker	350 k	97.5%
LAr EM Calorimeter	170 k	99.9%
Tile calorimeter	9800	99.5%
Hadronic endcap LAr calorimeter	5600	99.6%
Forward LAr calorimeter	3500	99.8%
LVL1 Calo trigger	7160	100%
LVL1 Muon RPC trigger	370 k	98.4%
LVL1 Muon TGC trigger	320 k	100%
MDT Muon Drift Tubes	350 k	99.7%
CSC Cathode Strip Chambers	31 k	97.7%
RPC Barrel Muon Chambers	370 k	93.8%
TGC Endcap Muon Chambers	320 k	99.7%



Cross Checks: Subtraction



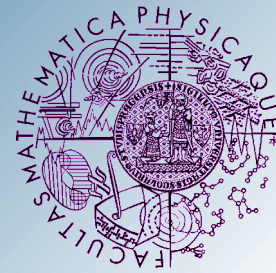
- Mean subtracted energy as a function of asymmetry



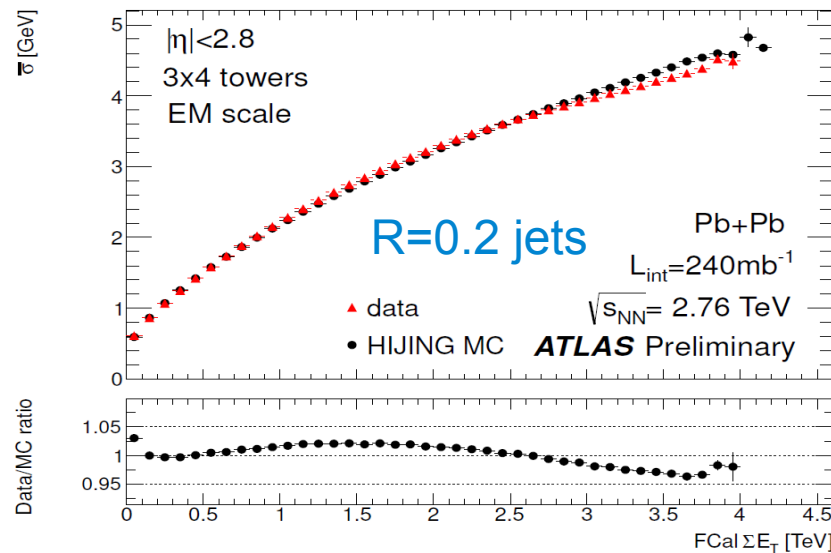
- no asymmetry dependence
- amount of subtracted energy for leading and sub-leading jet is comparable



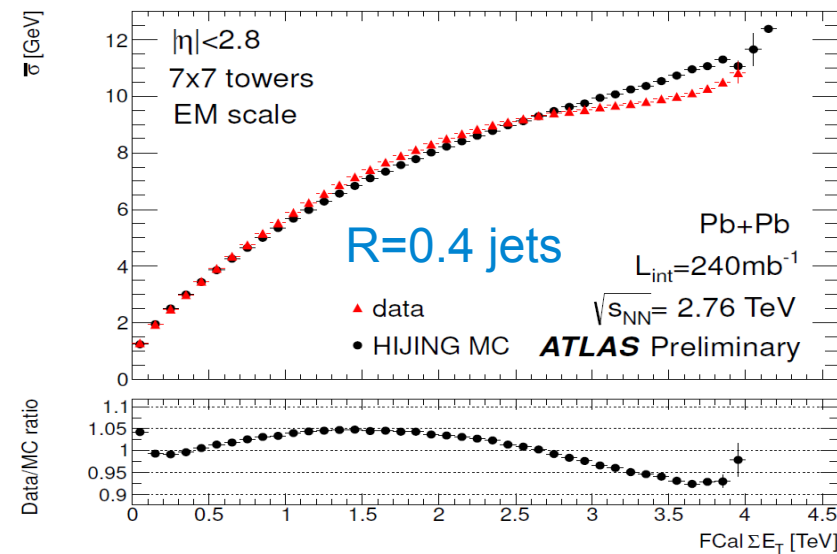
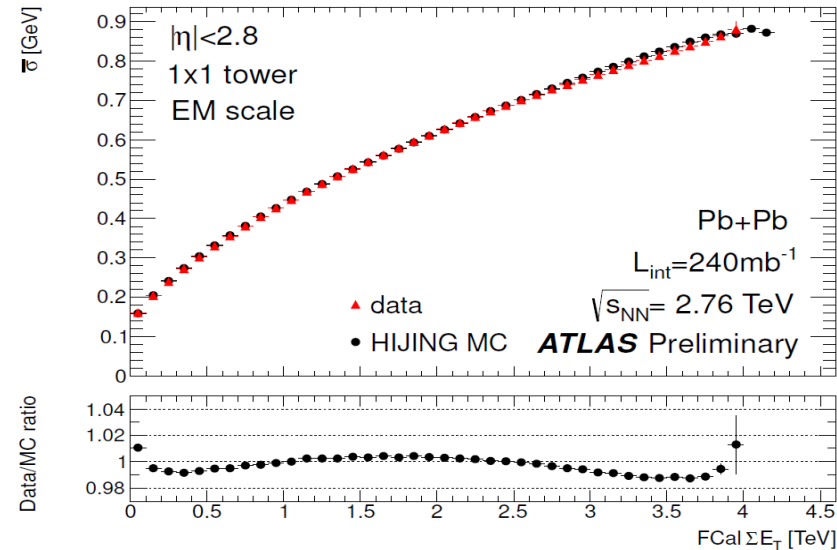
Background Fluctuations



- The fluctuations are evaluated as a standard deviation of the summed E_T in windows of towers of different size.
- 7x7 towers $\sim R = 0.4$ jets.
- 4x3 towers $\sim R = 0.2$ jets.

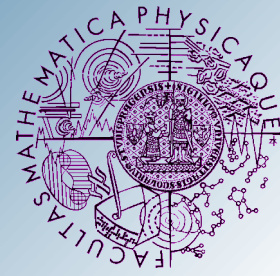


- Good agreement between data and MC.
- Basic data driven check of jet energy resolution.





Jet Reconstruction at ATLAS



- Reconstruction algorithm anti- k_t with $R=0.2, 0.3$ and 0.4 .
- Input: calorimeter towers 0.1×0.1 ($\Delta\eta \times \Delta\phi$).
- Event-by-event background subtraction:

$$E_{T_j}^{\text{sub}} = E_{T_j} - A_j \rho_i(\eta_j) (1 + 2v_{2i} \cos [2(\phi_j - \Psi_2)])$$

- ➡ Anti- k_t reconstruction prior to a background subtraction.
- ➡ Underlying event estimated for each longitudinal layer and η slice separately.
- We exclude jet candidates with $D = E_{T_{tower}}^{\text{max}} / \langle E_{T_{tower}} \rangle > 4$ to avoid biasing subtraction from jets **but no jet rejection based on D** .
- Additional iteration step to remove residual effect of the jets on the background estimation.
- Jets corrected for flow contribution.

Transverse Energy in 7x7 tower window

